

# Supplementary Material of “Semi-Supervised Video Deraining with Dynamical Rain Generator”

Zongsheng Yue<sup>1</sup>, Jianwen Xie<sup>2</sup>, Qian Zhao<sup>1</sup>, Deyu Meng<sup>1,3,\*</sup>

<sup>1</sup>Xi’an Jiaotong University, Xi’an, China

<sup>2</sup>Cognitive Computing Lab, Baidu Research, Bellevue, USA

<sup>3</sup>The Macau University of Science and Technology, Macau, China

zsyam@gmail.com, jianwen@ucla.edu, timmy.zhaoqian@gmail.com, dymeng@mail.xjtu.edu.cn

<https://github.com/zsyOAOA/S2VD>

## Abstract

*In this supplementary material, we provide more details on how to apply the proposed dynamic rain generator to synthesize new rainy videos that look similar to any observed video, which only contains the rain layer. Rain generation experiments are also conducted to evaluate its effectiveness. Besides, more analysis about the model capacity and running time of our method are also presented to verify its superiority.*

## 1. Dynamical Rain Generator

In Sec. 3.1 of the main text, we design the following dynamical rain generator, i.e.,

$$\mathbf{s}_t = F(\mathbf{s}_{t-1}, \mathbf{z}_t; \boldsymbol{\alpha}), \quad (1)$$

$$\mathcal{R}_t = H(\mathbf{s}_t; \boldsymbol{\beta}), \quad (2)$$

where

$$\mathbf{z}_t \sim \mathcal{N}(0, \mathbf{I}), \quad \mathbf{s}_0 \sim \mathcal{N}(0, \mathbf{I}). \quad (3)$$

The detailed explanations about Eqs. (1)-(3) can be seen in the main text. By denoting  $\mathbf{z} = \{\mathbf{z}_t\}_{t=1}^n$  and  $\boldsymbol{\theta} = \{\boldsymbol{\alpha}, \boldsymbol{\beta}\}$ , Eqs. (1) and (2) can be simply written together as follows,

$$\mathcal{R} = G(\mathbf{s}_0, \mathbf{z}; \boldsymbol{\theta}). \quad (4)$$

### 1.1. Maximum Likelihood Estimation

Given any observed video  $\mathcal{R}^o$  purely containing rain layer, we assume that it is generated by the aforementioned generator with an additional residual term  $\mathcal{E}$ , i.e.,

$$\begin{aligned} \mathcal{R}^o &= G(\mathbf{s}_0, \mathbf{z}; \boldsymbol{\theta}) + \mathcal{E}, \\ \mathcal{E}_{ijt} &\sim \mathcal{N}(0, \sigma^2), \end{aligned} \quad (5)$$

\*Corresponding author.

---

**Algorithm 1** Inference and learning procedure for the dynamic rain generator

---

**Input:** Observe data  $\mathcal{R}^o$ , number of Langevin steps  $l$ .

**Output:** the generator parameters  $\boldsymbol{\theta}$ .

- 1: Initialize  $\boldsymbol{\theta}$ .
  - 2: **while** not converged **do**
  - 3:   **E-Step:** Run  $l$  steps of Langevin dynamics to sample  $\mathbf{z}$  following Eq. (7).
  - 4:   **M-Step:** Update  $\boldsymbol{\theta}$  by gradient descent in Eq. (10).
  - 5: **end while**
- 

where  $\mathcal{E}_{ijt}$  denotes the element with index  $(i, j, t)$  in  $\mathcal{E}$ .

According to Eq. (5), our goal turns to maximize the log-likelihood  $p(\mathcal{R}^o; \boldsymbol{\theta})$  w.r.t. the parameters  $\boldsymbol{\theta}$ , i.e.,

$$\begin{aligned} \max_{\boldsymbol{\theta}} \log p(\mathcal{R}^o; \boldsymbol{\theta}) &= \log \int p(\mathcal{R}^o | \mathbf{z}) p(\mathbf{z}) d\mathbf{z} \\ &= \log \int \mathcal{N}(G(\mathbf{s}_0, \mathbf{z}; \boldsymbol{\theta}), \sigma^2 \mathbf{I}) p(\mathbf{z}) d\mathbf{z} \\ &\triangleq \mathcal{L}(\mathcal{R}^o; \boldsymbol{\theta}), \end{aligned} \quad (6)$$

where  $p(\mathbf{z})$  is defined in Eq. (3).

### 1.2. Inference and Learning Algorithm

Inspired by the technology of alternative back-propagation through time [6], a Monte Carlo-based EM [2] algorithm is designed to learn the model parameter  $\boldsymbol{\theta}$  by solving the problem of Eq. (6), which consists of two alternative steps, i.e., one expectation step and one maximization step. The expectation step aims to sample latent variable  $\mathbf{z}$  from the posterior  $p(\mathbf{z} | \mathcal{R}^o)$ , while the maximization step updates the parameters  $\boldsymbol{\theta}$  based on the current sampled  $\mathbf{z}$ .

**E-Step:** Let  $\boldsymbol{\theta}^{\text{old}}$  and  $p_{\text{old}}(\mathbf{z} | \mathcal{R}^o)$  denote the current parameters  $\boldsymbol{\theta}$  and the corresponding posterior distribution, we can sample  $\mathbf{z}$  from  $p_{\text{old}}(\mathbf{z} | \mathcal{R}^o)$  using the Langevin dynam-

ics [3]:

$$\begin{aligned} \mathbf{z}^{(\tau+1)} &= \mathbf{z}^{(\tau)} + \frac{\delta^2}{2} \left[ \frac{\partial}{\partial \mathbf{z}} \log p_{\text{old}}(\mathbf{z} | \mathcal{R}^o) \right] \Big|_{\mathbf{z}=\mathbf{z}^{(\tau)}} + \delta \boldsymbol{\xi}^{(\tau)} \\ &= \mathbf{z}^{(\tau)} - \frac{\delta^2}{2} \left[ \frac{\partial}{\partial \mathbf{z}} g(\mathbf{z}) \right] \Big|_{\mathbf{z}=\mathbf{z}^{(\tau)}} + \delta \boldsymbol{\xi}^{(\tau)}, \end{aligned} \quad (7)$$

where

$$g(\mathbf{z}) = \frac{1}{2\sigma^2} \left\| \mathcal{R}^o - G(\mathbf{z}, \mathbf{s}_0; \boldsymbol{\theta}^{\text{old}}) \right\|_2 + \frac{1}{2} \|\mathbf{z}\|_2, \quad (8)$$

$\tau$  indexes the time step for Langevin dynamics,  $\delta$  denotes the Langevin step size. And  $\boldsymbol{\xi}^{(\tau)}$  is the Gaussian white noise, which is added to prevent trapping into local modes. A key point in Eq. (7) is  $\frac{\partial}{\partial \mathbf{z}} \log p_{\text{old}}(\mathbf{z} | \mathcal{R}^o) = \frac{\partial}{\partial \mathbf{z}} \log p_{\text{old}}(\mathcal{R}^o, \mathbf{z})$ , and the right term can be easily calculated.

In practice, for the purpose of avoiding high computational cost of MCMC, Eq. (7) is initialized with the previous updated result of  $\mathbf{z}$  at each iteration. As for the initialized state vector  $\mathbf{s}_0$  of Eq. (5), we also sample it together with  $\mathbf{z}$  using the Langevin dynamics.

**M-Step:** Denote the sampled latent variable in E-Step as  $\tilde{\mathbf{z}}$ , M-Step aims to maximize the approximate upper bound w.r.t. parameters  $\boldsymbol{\theta}$  as follows:

$$\begin{aligned} \max_{\boldsymbol{\theta}} \mathcal{Q}(\boldsymbol{\theta}) &= \int p_{\text{old}}(\mathbf{z} | \mathcal{R}) \log p(\mathcal{R}^o, \mathbf{z}; \boldsymbol{\theta}) d\mathbf{z} \\ &\approx \log p(\mathcal{R}^o, \tilde{\mathbf{z}}; \boldsymbol{\theta}). \end{aligned} \quad (9)$$

Equivalently, Eq. (9) can be further rewritten as the following minimization problem, i.e.,

$$\min_{\boldsymbol{\theta}} \hat{\mathcal{L}}(\boldsymbol{\theta}) = \frac{1}{2\sigma^2} \left\| \mathcal{R}^o - G(\tilde{\mathbf{z}}, \mathbf{s}_0; \boldsymbol{\theta}) \right\|_2.$$

Naturally, we can update  $\boldsymbol{\theta}$  by gradient descent based on the back-propagation (BP) algorithm [5] as follows,

$$\boldsymbol{\theta} \leftarrow \boldsymbol{\theta} - \eta \frac{\partial}{\partial \boldsymbol{\theta}} \hat{\mathcal{L}}(\boldsymbol{\theta}), \quad (10)$$

where  $\eta$  denotes the step size. A detailed description of our entire algorithm is presented in Algorithm 1.

## 2. Rain Generation Experiments

### 2.1. Evaluation on Rain Generation Task

Given any video purely containing a rain layer, the proposed dynamic rain generator is able to learn the underlying dynamics of rains from the video. After that, with the trained generator, we can not only recover the original rain video but also generate many new realistic rain layers. To verify this point, one rain layer video synthesized by the commercial Adobe After Effects<sup>1</sup> is downloaded from

<sup>1</sup><https://www.adobe.com/products/aftereffects.html>

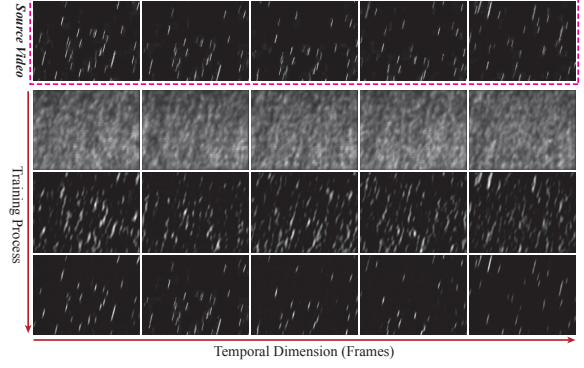


Figure 1. An illustration of the source and recovered rain videos. From top to bottom: the 1st row is the source rain video, and the 2-4th rows are the recovered ones by our learned dynamic rain generator after 3, 10 and 20 iterations. From left to right, 5 adjacent image frames in each video are displayed.

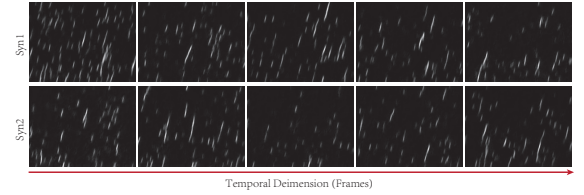


Figure 2. Two typical examples of generated rain videos by the learned dynamic rain generator are shown, and each row corresponds to a different initialization of  $\mathbf{s}_0$  and  $\{\mathbf{z}_t\}$ .

YouTube as a source video. We learn a dynamic rain generator from this video, and the visualization of recovered rain video by our generator at different iterations are displayed in Fig. 1. It can be seen that our generator can quickly recover the rain layers of all image frames in the video only with 20 iterations, which demonstrates its representation power in this task.

Additionally, two synthesized rain videos by the learned generator are shown in Fig. 2. To generate such videos, we only need to randomly initialize the state variable  $\mathbf{s}_0$  and the innovation vectors  $\{\mathbf{z}_t\}$  in Eq. (1) from Gaussian distribution, and then follow Eqs. (1) and (2) to output a sequence of image frames. The vivid rain videos shown in Fig. 2 indicate that our generator indeed captures the intrinsic generative laws underlying the source video. Therefore, it can be used to represent the rain layers in our proposed deraining framework presented in Sec. 3.1 of the main text.

### 2.2. User Study

While we have displayed the synthesized rain layers by our dynamic generator in Fig. 2, now a user study is further conducted to quantitatively evaluate their realism. Three currently widely-used benchmark data sets are considered as compared methods, including *RainSynComplex25* [4], *RainSynLigh25* [4] and *NTURain* [1]. The rain layers of

Table 1. Quantitative results of user study experiments on different rain video clips.

Metrics	Methods				
	<i>RainSynComplex25</i>	<i>RainSynLigh25</i>	<i>NTURain</i>	Adobe	Ours
Rating $\uparrow$	1.30 $\pm$ 0.66	2.72 $\pm$ 0.98	3.49 $\pm$ 1.02	4.02 $\pm$ 0.84	4.04 $\pm$ 0.82
Realism $\uparrow$	26.04	54.34	69.81	80.38	80.75

Table 2. A comparison of the number of model parameters (K) and running time (s) among different methods.

Metrics	Methods				
	DDN	PReNet	SpacCNN	SLDNet	S2VD
# Parameters (K)	57	169	477	166302	525
Time (s)	0.035	0.187	3.632	2.268	0.032

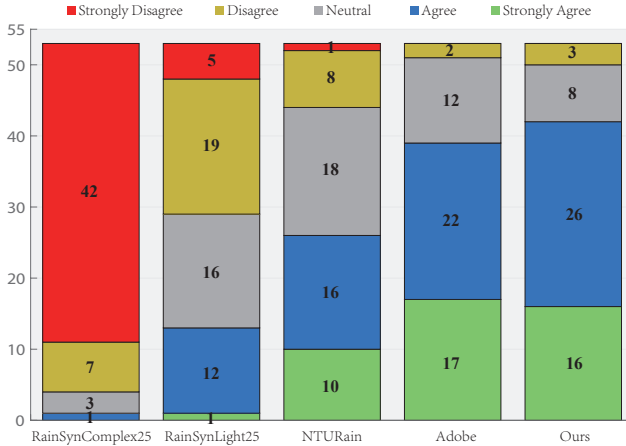


Figure 3. User study of rain realism. The  $y$ -axis represents the rating of the statement *Rain in the video clip looks realistic*. Our generated rain layers are even a little bit better than those of the commercial Adobe After Effects.

them are obtained as follows,

$$\mathcal{R} = \max_c(\mathcal{Y} - \mathcal{X}), \quad (11)$$

where  $\mathcal{Y}$  and  $\mathcal{X}$  denote the rainy video and the corresponding clean video, respectively,  $\max_c(\cdot)$  is the element-wise maximization operation along the channel dimension (RGB). Besides, since our generator is trained on one source video downloaded from YouTube, which is produced by the commercial Adobe After Effects<sup>2</sup>, thus we also regard it as one compared method.

For visual comparisons, some typical image frames of these four rain videos and the synthesized rain video by our generator are shown in Fig. 4. To evaluate their realism, we present these five video clips in a random order, each with 100 continuous frames, to 53 recruited participants, and then ask each of them to rate how real every video clip is, using a 5-point Likert scale. Therefore, we finally get 53 ratings for each video clips as shown in Fig. 3. And the corresponding mean ratings and realism scores are list in Table 1, in which the realism scores are calculated by converting the ratings to the range [0,1]. It can be easily seen that

<sup>2</sup><https://www.adobe.com/products/aftereffects.html>

the video clips generated by our proposed generator achieve the best results, even a little bit better than that of the commercial Adobe After Effects software, which indicates the effectiveness of our dynamic rain generator. Therefore, it is promising and reasonable to use this dynamic generator to fit the rain layers in our proposed video deraining method of the main text.

### 3. Model capacity and running time of S2VD

In this part, we compare the model capacity (number of model parameters) and running time of different deep learning (DL)-based methods. For the number of parameters of the proposed S2VD, we only consider the parameters in the derainer  $f(\cdot; W)$ , since only the derainer is desired in the testing phase after training. The running time evaluation was performed on a computer with 6-cores Inter(R) Core(TM) i7-8700K CPU (3.3GHz) and a Nvidia GTX 1080Ti GPU. Specifically, it is tested on a rainy video that contains 60 image frames with spatial size  $480 \times 640$  pixels, and the average time on each frame is regarded as the running time for each method. And the time for data transfer between CPU and GPU is not counted during calculation.

The results are listed in Table 2. We observe that: 1) On the whole, the video deraining methods have more parameters than the single image deraining methods. Comparing with two state-of-the-art video deraining methods, the number of parameters of our S2VD is very close to SpacCNN and about 300 times smaller than SLDNet. 2) As for the running time, our S2VD is at least 70 times faster than SLDNet and SpacCNN, which is mainly because our model uses a simple architecture for the derainer network. Considering the superiorities in both model capacity and running time, S2VD is very competitive and appealing for real applications.

### References

- [1] Jie Chen, Cheen-Hau Tan, Junhui Hou, Lap-Pui Chau, and He Li. Robust video content alignment and compensation for rain removal in a cnn framework. In *Proceedings of the IEEE Conference on Computer Vision and Pattern Recognition (CVPR)*, pages 6286–6295, 2018. 2
- [2] Arthur P Dempster, Nan M Laird, and Donald B Rubin. Maximum likelihood from incomplete data via the em algorithm. *Journal of the Royal Statistical Society: Series B (Methodological)*, 39(1):1–22, 1977. 1
- [3] Paul Langevin. On the theory of brownian motion. 1983. 2

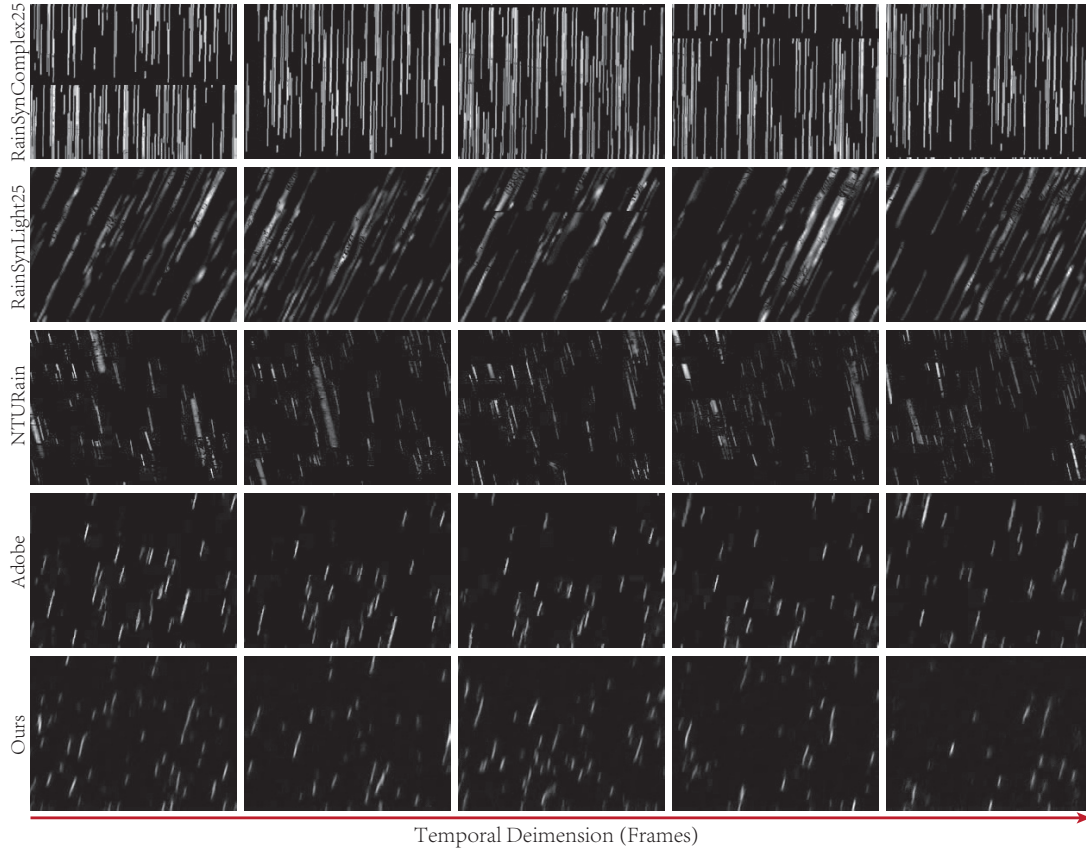


Figure 4. Visualization of the rain layers in different data sets. From top to bottom: the rain layers contained in *RainSynComplex25*, *RainSynLigh25* and *NTURain*, the rain layers generated by Adobe After Effects and our trained dynamic rain generator.

- [4] Jiaying Liu, Wenhan Yang, Shuai Yang, and Zongming Guo. Erase or fill? deep joint recurrent rain removal and reconstruction in videos. In *Proceedings of the IEEE Conference on Computer Vision and Pattern Recognition (CVPR)*, pages 3233–3242, 2018. **2**
- [5] David E Rumelhart, Geoffrey E Hinton, and Ronald J Williams. Learning representations by back-propagating errors. *nature*, 323(6088):533–536, 1986. **2**
- [6] Jianwen Xie, Ruiqi Gao, Zilong Zheng, Song-Chun Zhu, and Ying Nian Wu. Learning dynamic generator model by alternating back-propagation through time. In *Proceedings of the AAAI Conference on Artificial Intelligence (AAAI)*, volume 33, pages 5498–5507, 2019. **1**